Available online at www.sciencedirect.com
SCIENCE DIRECT®
Vision Research 45 (2005) 1755–1768
Vision Research
www.elsevier.com/locate/visres

Alteration of the perceived path of a non-pursued target during smooth pursuit: Analysis by a neural network model

Moran Furman, Moshe Gur *

Department of Biomedical Engineering, Technion, Israel Institute of Technology, Haifa 32000, Israel

Received 20 November 2003; received in revised form 17 December 2004

Abstract

During pursuit of a circularly moving target, the perceived movement of a second circularly moving target is altered. The perceived movement of the non-pursued target is different from both its real movement path and its retinal path. In the present paper this phenomenon is studied using a physiologically based neural network model. Simulation results were compared to psychophysical findings in human subjects. Model simulations enabled us to suggest an explanation for this phenomenon in terms of underlying physiological mechanisms and to estimate the contribution of the efferent eye-movement signal to the perceptual process.

Keywords: Pursuit eye movement; Neural network; Motion perception; Area MST

1. Introduction

The highly developed smooth pursuit system enables primates and humans to keep the image of a moving object on the fovea at objects speed up to 30°/s. During pursuit, objects movements on the retina are different from their real world movements, forcing the visual system to use some kind of eye-movements compensation to enable us to perceive, for example, a pursued object as moving, although its retinal image is nearly stable.

Early theories of eye-movement compensation (Gregory, 1958; Von Helmholtz, 1909; Von Holst, 1954), suggested that extraretinal information, a copy of the motor command sent to the eyes, is subtracted from the retinal information on target velocity. Various physiological and psychophysical studies are consistent with this mechanism, and it is thus commonly assumed that perception during pursuit eye movements involves a combination of afferent (visual) and efferent (motor) signals.

Basic perceptual phenomena related to pursuit were successfully addressed by theoretical studies of the subject (see Pack, Grossberg, & Mingolla, 2001). More complex phenomena (see below), however, still lack theoretical analysis. In Furman and Gur (2003) we described a physiologically based neural network model for motion processing in the cortex during pursuit. The model was based on single cell properties and on organization of relevant cortical areas. The model analyzed integration of afferent and efferent signals within a broad context including a full representation of directions and velocities of movement, and complex retinal images. Therefore our model enables, for the first time, analysis of complex perceptual phenomena related to pursuit. Section 3 gives a brief description of the model.

This work deals with two issues not treated by previous models; the effectiveness of efferent vs. afferent signals and the physiological mechanisms underlying complex perceptual phenomena related to smooth pursuit.

* Corresponding author. Tel.: +972 4 8294116; fax: +972 4 8294566.
E-mail address: mogi@bm.technion.ac.il (M. Gur).

0042-6989/$ - see front matter © 2005 Elsevier Ltd. All rights reserved.
doi:10.1016/j.visres.2004.12.012

There is an ongoing debate on the degree of effectiveness of the efferent signal in the perceptual process. It is commonly assumed that the efferent signal is less effective than the afferent one, as demonstrated, for example, by the underestimation of target speed during pursuit (the *Aubert–Fleich phenomenon*, Aubert, 1886) and the perceived movement of a stationary background (the *Filehne effect*, Filehne, 1922). Some researchers suggested that the efferent signal participates in a significant manner in the perceptual process (e.g. Carr, 1935; Mack & Herman, 1972), while others claimed that the efferent signal contribution is marginal (e.g. Dodge, 1910; Festinger, Sedgwick, & Holtzman, 1976; Stoper, 1973).

That there is a complex interaction between efferent and afferent signals during pursuit is evident in a family of perceptual phenomena: The alteration in the apparent trajectory of a moving target while a second one is being pursued (Dodge, 1904, 1910). The present work focuses on the perceived path of a circularly moving target during pursuit of another, circularly moving, one. This phenomenon was first described by Kano and Hayashi (1981) who reported that the perceived path of the non-tracked spot differed dramatically from its retinal path—particularly for spots moving, out of phase, in opposite directions.

To enable a more detailed and quantitative comparison between simulation results and experimental data, we studied the phenomenon described by Kano and Hayashi (1981) for a greater number of subjects and different parameter values.

We show that the model suggests an explanation for the perceptual phenomena in terms of physiological mechanisms, and accounts for experimental data if the efferent signal is assumed to significantly participate in the perceptual process, at about 80% strength relative to the visual signal.

2. Experimental methodology

2.1. Subjects

Eight subjects (4 males, 4 females, ages 24–57), including the 2 authors, took part in all experiments. All had normal or corrected-to-normal vision. Three subjects were naive about the purpose of the experiment.

2.2. Apparatus

Stimuli were generated using a 1.80 GHz Pentium PC and displayed on an SVGA monitor with a 600×800 pixel resolution at a 85 Hz frame rate. The monitor was viewed binocularly at a distance of 70 cm in a darkened room. A chin rest restricted the subjects' head movements.

2.3. Stimuli

Each test stimulus consisted of a pair of circularly moving spots. The 3 mm diameter spots were moderately dim but distinctly visible. Both spots moved at the same angular velocity (3.5 rad/s), along equi-diameter (9 cm) circles whose centers were separated by 12 cm in the horizontal direction. At the beginning of each stimulus, the left spot (target A) appeared first, moving clockwise. After completing one cycle, the right spot (target B) appeared and moved with target A until completing 4 additional cycles. Target B moved either in the same direction as target A (clockwise) or in the opposite direction (counterclockwise). Phase differences between targets were 0°, 60°, 120°, or 180°. The eight combinations of movement directions and phase differences were presented in a random order.

An additional stimulus was used as a reference; it consisted of a stationary spot (target A) and a circularly moving spot. The spots' characteristics were as described above, only that target A was now stationary at the center of its previous path.

2.4. Procedure

When viewing the two moving spots, each subject was instructed to track target A as accurately as possible during the whole presentation and memorize the perceived path of target B. After the presentation, the subject was requested to verbally report the shape of target B perceived path (e.g. a tilted elongated ellipse) and then a small circle appeared around the center of target B path. Control keys enabled the subject to change the circle size, or to transform it to an ellipse of varying size, axes ratio, and inclination. The subject thus adjusted the curve presented on the screen according to the memorized target B path. The subject could choose to repeat the last stimulus presentation and in this case, after the presentation, the ellipse appeared as last modified by him. The subject could then modify it further, or leave it as is, and move to the next trial or repeat the procedure. A record of the last ellipse estimation (axes and inclination) at each session was stored.

To use the reference stimulus, depicting a stationary target A with a moving target B, the subjects were instructed to fixate on the stationary target during the whole presentation and memorize the perceived path of the moving one. After the presentation the subjects recorded the perceived path of the non-pursued target by the above described procedure.

2.5. Eye-movement monitoring

A control experiment with 4 of the 8 subjects was performed to monitor the subjects' eye movement during pursuit. The viewing conditions and experimental setup

were the same as described above. During pursuit of the circularly moving target, eye position was measured using an ASL eye-tracker (model 504) with a 60 Hz sampling frequency.

2.6. Experimental data analysis

First, the perceived movement paths as reported by each subject were scaled and normalized according to the subject's perceived movement path size during fixation. Path size was defined as approximately the ellipse perimeter

$$L = 2\pi\sqrt{\frac{1}{2}(a^2 + b^2)} \tag{1}$$

where a and b are the ellipse axes. Next, for each stimulus condition, the perceived movement paths as reported by all subjects were plotted around the planar axes origin. To estimate a mean movement path, a best-fit ellipse was numerically calculated. For this purpose, we defined the "distance" between two ellipses by summing their differences along all radial directions. The best fit was defined as the ellipse with axes A, B and inclination Θ minimizing the functional $u(A, B, \Theta)$, indicating the total distance to the perceived ellipses

$$u(A, B, \Theta) = \sum_{k=1}^{n} \int_0^{2\pi} [r_k(\theta) - R(\theta)]^2 \mathrm{d}\theta \tag{2}$$

where

$$R(\theta) = \left(\sqrt{\frac{\cos^2(\theta - \Theta)}{A^2} + \frac{\sin^2(\theta - \Theta)}{B^2}} \right)^{-1} \tag{3}$$

and

$$r_k(\theta) = \left(\sqrt{\frac{\cos^2(\theta - \theta_k)}{a_k^2} + \frac{\sin^2(\theta - \theta_k)}{b_k^2}} \right)^{-1} \tag{4}$$

a_k and b_k indicate the long and short axes of the experimental paths, respectively, and θ_k their inclinations.

Eye movements during 128 cycles of target movement (8 sessions for each of the 4 subjects, 4 cycles in each session) were analyzed. Pursuit during the first cycle of target A (before the appearance of target B) was excluded from the analysis (see Section 2.3). In 13 cases, saccades with amplitudes >2° and velocities >50°/s were observed. The 13 cycles including these saccades were excluded from the 128 cycles data pool. Horizontal and vertical pursuit gains were measured by comparing eye velocity with target velocity.

3. Model

3.1. Review of the neural network

The model was a feed-forward neural network, with three layers of computational units, simulating neurons at three cortical areas in the motion processing stream. Fig. 1 depicts the general structure of the model. The activity of each model unit was an analog, non-linear threshold function of its total input. Connections between every two network layers were separated into excitatory and inhibitory ones.

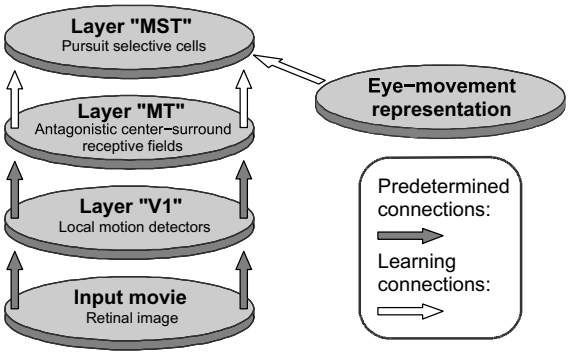

Fig. 1. General structure of the network model (from Furman & Gur, 2003). The input movie, representing the dynamic retinal image, is processed first by V1 units selective to local movements in a specific direction and velocity within their receptive-field (RF). The units in the next processing layer, representing MT, have antagonistic center–surround RFs. The third layer, MST, receives, in addition to visual input arriving through MT, an extra-retinal input representing eye-movement direction and velocity.

The input to the first layer was a movie representing the retinal image. The 6504 units in the first processing layer simulated direction selective cells in the primary visual cortex (V1), which respond selectively to local movement within their RF. Direction selectivity of V1 units was modeled using the delayed inhibition approach, and velocity selectivity was modeled by a Gaussian function of the average velocity within their RF (for details, see Appendix A.3 in Furman & Gur, 2003).

The second processing level, containing 3048 units, simulated center–surround RF organization of neurons in cortical area MT. The number of MT units is larger in the present simulations than in Furman and Gur (2003), since MT units here have smaller RFs to enable a more detailed representation of the visual field by the MT layer. Center–surround RF organization was implemented by constructing appropriate connections between V1 and MT units. MT velocity selectivity was modeled explicitly, by setting the V1–MT connections to yield different velocity response curves characteristic of physiological foveal MT units (for details, see Appendix A.4 in Furman & Gur, 2003).

The third layer modeled a sub-population of medial-superior-temporal (MST) area pursuit selective cells. This layer contained 300 units, receiving both a visual input from MT units and an extra-retinal input representing eye movements.

3.2. Training of the network

Connections between MT and MST model layers were not predetermined, but developed via an unsupervised learning process, as were the connections between the eye-movement representation units and MST. At the beginning of the training period all connection weights were relatively weak and random. Therefore MST units did not perform any specific function. At each training step, weights were updated according to the network units' activities. Different training rules were used for excitatory and inhibitory connections ("synapses"), reflecting the different functionalities of these synapses.

For training the excitatory connections, we used Oja's rule (Oja, 1982), a modification of Hebbian learning (Hebb, 1949), that favors correlated activity between pre- and post-synaptic neurons. The momentary connection-weight change, $\Delta w_{ij}^{\text{exc}}$, between a neuron with activity level a_i, and a neuron with activity level a_j, is

$$\Delta w_{ij}^{\text{exc}} = \varepsilon_{\text{exc}} a_j (a_i - w_{ij} a_j) \tag{5}$$

where ε_{exc} determines the learning rate of the excitatory synapses.

In contrast to excitatory synapses, inhibitory synapses reduce, on average, the correlation between pre- and post-synaptic neurons' activities. Therefore, for the inhibitory synapses we constructed a learning rule favoring anti-correlation between the activity of pre- and post-synaptic neurons

$$\Delta w_{ij}^{\text{inh}} = \varepsilon_{\text{inh}} \left[(1-\lambda)(\hat{a}_i - \hat{a}_j)^2 - \lambda(\hat{a}_i + \hat{a}_j - 1)^2 + \lambda \right] \tag{6}$$

where $\hat{a}_i$ and $\hat{a}_j$ are the normalized firing rates of the two neurons (their value is between 0 and 1). The normalization is performed over the population of the neurons in the layer they belong to. ε_{inh} determines the learning rate of the inhibitory synapses, and λ was set to 0.7.

The network was trained on a sequence of input patterns representing periods of pursuit eye movements. In each input pattern, a pursued target was moving against a textured background, in one of the possible directions and velocities of movement. The total-weight-change-rate during training was used to assess convergence and terminate the training process.

3.3. Review of post-training MST response properties

In Furman and Gur (2003) we tested the responses of post-training MST units to a target moving linearly in different directions and velocities, both during fixation (no extra-retinal input) and during pursuit.

Most post-training MST units were directional, and their preferred directions in the two stimulus conditions were nearly the same (see Fig. 11 in Furman & Gur, 2003). MST units were also tuned to velocity of movement (Fig. 13 in Furman & Gur, 2003). Most MST units had either low-pass or high-pass velocity tuning. The types of velocity responses during fixation and during pursuit were correlated. There is relatively little physiological data on velocity response properties of MST units. According to some studies, during fixation most MST units show a graded response to velocity, while units having low-pass type of velocity preference are infrequently observed (Kawano, Shidara, Watanabe, & Yamane, 1994; Tanaka, Sugita, Moriya, & Saito, 1993). Given the physiological data, only the high-pass MST units were selected for the model simulations.

3.4. Interpretation of MST population response to complex stimuli

The correlation between MST responses during fixation and during pursuit suggests that they may be interpreted as the physiological substrate of a single target's perceived movement in world-centered coordinates. In the present study we assumed MST responses to be the population coding of the perceived target's movement for complex stimuli as well (see Discussion, Section 5.2).

After training the network, we simulated the response of each MST unit to a single target moving linearly in different directions, and calculated the preferred direction of each unit. Then, given a complex stimulus, MST population response was decoded to obtain an estimated movement vector

$$\vec{v}_{\text{pop}} = \left(\sum_{k=1}^{N} R_k \cos \Phi_k, \sum_{k=1}^{N} R_k \sin \Phi_k \right) \tag{7}$$

where R_k is the response of MST unit k, and Φ_k its preferred direction of linear movement.

In the simulations we included only MST units with a high-pass velocity tuning. To simplify interpretation and analysis of MST population response, we approximated the velocity tuning of MST units by a linear function. Consequently, MST population average magnitude directly represented movement speed. We have also assumed that the angular velocity was constant in all stimulus conditions.

3.5. Simulating the perceived path of the non-pursued target

In the present study we use the model to simulate the perceived path of a target during pursuit of a second, circularly moving one. In real life, the brain recognizes the two dots as separate objects, and deals with responses to each. Since our model does not deal with object recognition, it can not assign the appropriate responses to each target. To be able to simulate re-

sponses resulting from the second, non-tracked, target, we eliminated the retinal image of the pursued target. That is, we simulated a hypothetical pursuit of a diminishingly small and dim target so the model MST population response can be interpreted directly in terms of the perceived movement of the non-pursued target. We assume that the perceived path shape of the non-pursued target is determined by integration of velocity signals represented by the MST population, and ignore the possible contribution of position information since unlike static shape perception, there is no clear physiological evidence of position signals contributing to shape perception during pursuit eye movements (see Discussion, Section 5.2).

3.6. Relation between efferent and afferent signals

In our model, as in physiological data, V1 and MT units response magnitude depends on stimulus attributes such as size or orientation. Therefore the relation between afferent (visual) and efferent (motor) signals converging on MST depends on both stimulus visual characteristics and the extra retinal command for execution of eye movements. The brain probably uses some kind of normalization while integrating both signals, otherwise perceived movement would have been dramatically dependent on stimulus features. In the present study the visual target is the same in all simulations—a one-pixel light point. The relation between efferent and afferent signals was calibrated by simulating MST responses to an input depicting a moving target during fixation (with only afferent signal active), and during stabilized pursuit (with only efferent signal active). The efferent and afferent signals were considered of equal magnitude if the same response was obtained during fixation and during pursuit.

4. Results

4.1. Preliminary example: A rotating target during fixation

We demonstrate our simulation procedure using a preliminary simple example: responses to a rotating target during fixation. Here, the input representing eye movements was inactive so that the only input MST units received was from the visual stream.

Fig. 2 shows three snapshots of the input movie used in the present example—a point target moving counterclockwise in a circular path (approximated by a hexagon).

The input movie was first processed by the V1 layer. Each V1 unit responded best to movement in its preferred direction within its RF. Fig. 3 shows three snapshots of V1 population response to the stimulus shown in Fig. 2, at corresponding time steps. V1 units were separated into six groups according to their directional preference. Within each group V1 units were retinotopically organized and the brightness of each unit represents its activity level. As can be seen, at each moment, V1 units responded to the moving object if it fell within their RF, and its movement direction was close to the units' preferred direction. The dynamic

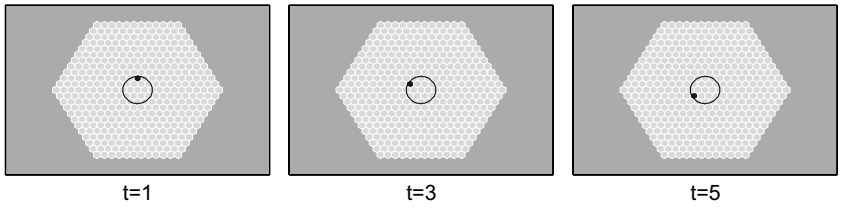

Fig. 2. Three snapshots of an input movie representing retinal image during fixation. A point target was moving counterclockwise in a circular path (approximated by a hexagon). Movement path is indicated in the image for clarity. The three snapshots correspond to time steps 1, 3 and 5.

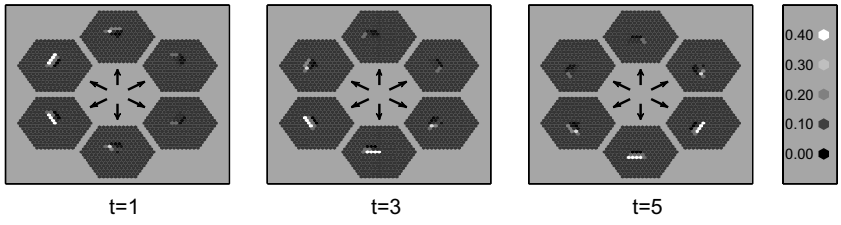

Fig. 3. V1 population response to a circularly moving object during fixation (Fig. 2). Each pixel represents a V1 unit, its brightness corresponding to its activity level (see scale). For simplicity, only V1 units with the same preferred velocity as the moving target's are shown. V1 units are separated into six groups, according to their direction preference. Each group is retinotopically organized, and within a group, all units have the same preferred direction of movement, indicated by the direction of the arrow pointing to the group. The snapshots correspond to the same time steps as in Fig. 2.

response of the V1 layer has a center of activity, shifting between sub-populations according to the target's position and direction of movement.

V1 activity served as an input to the next processing stage, MT. MT units had antagonistic center–surround RF organization with center and surround diameters 5 and 11 pixels, correspondingly. Fig. 4 shows snapshots of MT population response. MT units were excited when the moving object fell within their RF center and its movement direction was close to the units' preferred direction (bright areas), and were inhibited by movements in their RF surround (dark areas). Otherwise, MT units responded at their spontaneous activity level. MT center/surround organization was instrumental in MST training and is also important when textured rather than dark background is used.

MT units were connected to MST units of the third layer. As shown in Furman and Gur (2003), four classes of connections to MST were formed after training: excitatory and inhibitory MT to MST connections and excitatory and inhibitory eye-movement-units to MST connections.

These connection patterns determined MST direction selectivity such that, for example, the strongest excitatory connections of an MST unit selective to 0° movement during fixation were to MT units selective for the same direction and to inhibitory MT units selective for movement in the opposite direction (180°). Similar connection patterns were developed for this unit and eye-movement units; the strongest excitatory connections were to eye-movement units selective for 0° movements and the strongest inhibitory connections to eye-movement units selective for 180° movements (see Fig. 14 in Furman & Gur, 2003).

We show now MST units responses to a rotating target during fixation, and an interpretation of these responses in terms of object movements. In Fig. 5a, the response of each MST unit is represented by a line of corresponding length, drawn at the preferred direction of the unit. At each time step, the object's movement elicits a response in MST units with preferred directions close to the object's direction of movement. This population response was averaged to obtain a movement direction representation by MST. Fig. 5b shows the movement path obtained from integration of the movement vectors represented by MST. That is, each movement segment is drawn following the movement segment of the previous time step. As can be seen, the dynamic MST population response represents a movement along a nearly circular path, in accordance with the actual stimulus path.

4.2. Perceived path of a rotating target during circular pursuit in the same direction—simulation and psychophysical results

In this section we show results of tracking a spot (target A) describing a circular path in the dark while

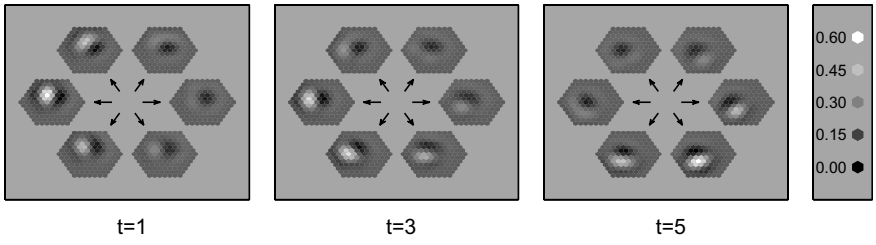

Fig. 4. MT population response to a circularly moving object during fixation (Fig. 2). The method of presentation is as in Fig. 3.

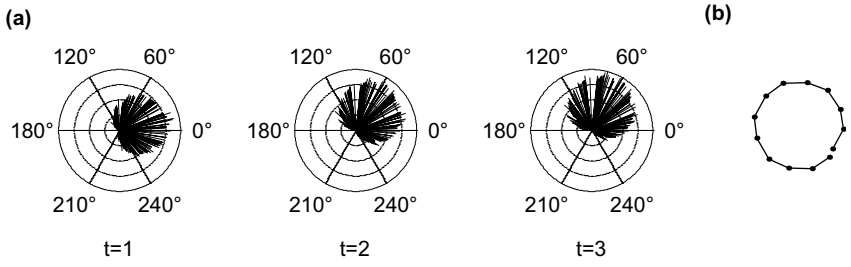

Fig. 5. (a) MST population response to a circularly moving object during fixation (Fig. 2), at three consecutive time steps. Each line represents an MST unit, its length and direction corresponding to the unit's response and preferred direction, respectively. Responses are normalized relative to maximal response. (b) Decoding of MST dynamic population response in term of movement path. The average vector of the population response is calculated at each time step. The resulting movement vectors are integrated to give a reconstructed movement path.

attending to a second spot (target B) moving at the same direction, angular velocity, and diameter as target A, but with various phase differences. Fig. 6a depicts the objective movement of the two targets. If pursuit is perfect, the retinal image of the non-pursued target (target B) is either stationary or moving along a circle (Fig. 6b). The circle diameter (D) depends on the phase difference between the two targets, according to

$$D = d\sqrt{1 - \cos\theta} \tag{8}$$

where d is the diameter of the real movement path of targets A and B, and θ is the phase difference.

During actual pursuit, however, the eyes do not follow the target movement perfectly. Therefore, we measured eye movements during pursuit of the circularly moving target (see Section 2.5). As shown in Table 1 the average horizontal and vertical gains during pursuit were 1.00 and 0.91 respectively. These results are in excellent agreement with Rottach et al. (1996) who found, for clockwise circular pursuit, horizontal and vertical gains of 0.97 and 0.89, respectively. A paired *t-test*, for the group of subjects as a whole, shows that the horizontal gain was significantly ($P < 0.05$) greater than the vertical one. This result is again consistent with Rottach et al. (1996).

Using the measured pursuit gains, we estimated the actual retinal path of the non-pursued target during tracking of the circularly moving spot. Fig. 6c depicts the estimated retinal path of the non-pursued target, based on the average horizontal and vertical components of pursuit gains.

Table 1
Summary of gain values during circular pursuit (mean ± s.d.)

Subject	Horizontal gain	Vertical gain
1	1.02 ± 0.03	0.99 ± 0.03
2	1.01 ± 0.04	0.93 ± 0.03
3	1.00 ± 0.05	0.88 ± 0.05
4	0.96 ± 0.06	0.83 ± 0.05

The estimated retinal paths depicted in Fig. 6c differ slightly from the idealized retinal paths of Fig. 6b. Since the over all gain is smaller than 1, and since the horizontal gain is somewhat larger than the vertical one, the paths are slightly elliptical, and their size is smaller than the idealized retinal path.

We constructed input movies representing retinal movement, and simulated the network response to phase differences of 0°, 60°, 120°, and 180°. Since pursuit gains were very close to 1, we assumed in the simulations that tracking of the pursued target was perfect. Using the actual retinal paths would have required exquisite spatial resolution for generating deformed movement paths, which would have greatly complicated the simulations. In the following simulations, we assumed that the efferent signal was 80% of the afferent one (see below). Fig. 7 shows, as an example, MST population response at six simulation time steps, at a 180° phase difference. MST population response was interpreted in terms of target

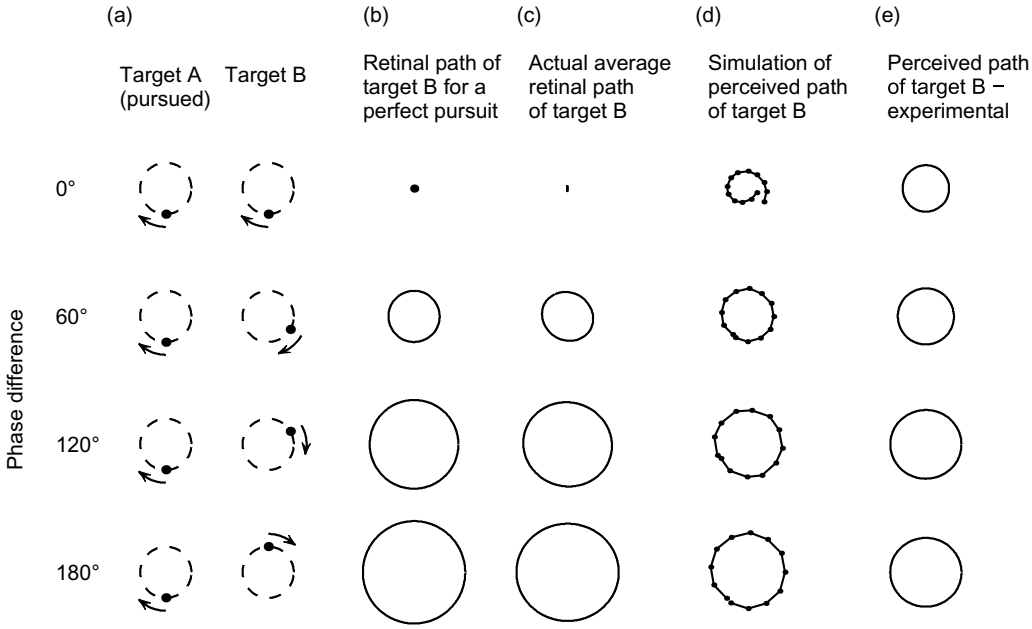

Fig. 6. Perceived movement path of a circularly moving spot during pursuit of a second spot moving in the same direction. (a) Objective movement of the two spots. Spot (target) A (pursued) moves counterclockwise along a circular path. Target B (non-pursued) moves in the same direction but with different phase lags along a circle of the same size. (b) Retinal image movement of target B for a perfect pursuit. (c) Estimated actual retinal image movement of target B, calculated according to average experimental pursuit gains. (d) Simulated movement path of target B represented by the MST population. (e) Experimental results of perceived movement of target B.

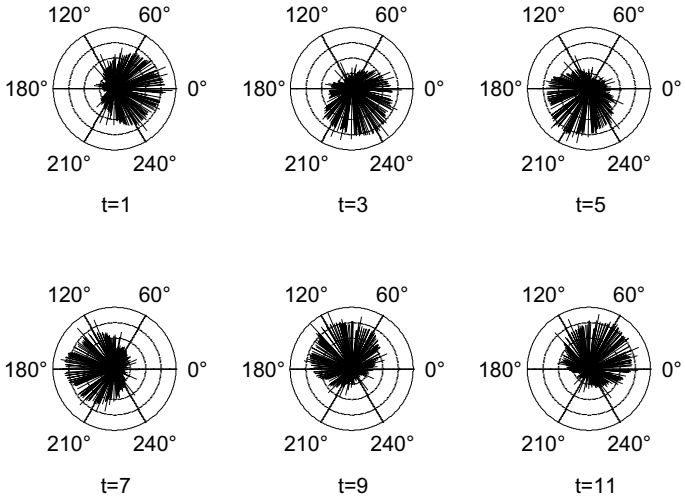

Fig. 7. Simulated MST population response to a circularly moving target, at six different time steps, during pursuit of a second target moving in the same direction at a 180° phase difference. Responses are normalized relative to the maximal response.

B movement (see Section 3.5) and the resulting movement paths are shown in Fig. 6d.

Fig. 6e shows the mean perceived movement paths obtained in our experiments, according to the ellipses' axes and inclinations reported by the observers (see Section 2.6). In all cases, subjects reported perceiving target B as moving along a circle or an ellipse. As can be seen, the mean perceived path was nearly circular, its size monotonically increasing with phase difference. Simulation results (Fig. 6d) closely resemble experimental findings and clearly differed from the actual retinal paths at phase differences of 0°, 120°, and 180° (Fig. 6c).

Our experimental findings of perceived movement paths are in qualitative agreement with Kano and Hayashi (1981, experiment 2a) findings. They, however, reported that in most cases observers perceived target B as moving along a vertically elongated ellipse, although some occasionally perceived a horizontally elongated one. While some of our observers indeed perceived a vertically elongated ellipse, in many occasions the observers perceived a circle or a tilted ellipse in different orientations, and, on average, the perceived path was nearly circular with the ratio between the vertical and horizontal axes of the mean perceived path not significantly greater than 1 ($p < 0.05$).

4.2.1. The effect of changing the efferent to afferent signals ratio

In the simulations presented above we assumed that the efferent signal was 80% of the afferent one. We describe now the effect of changing the efferent signal strength. We define ω_{ef} as the ratio between the efferent and afferent signals. The previous simulations were repeated with four values of ω_{ef}: 0%, 40%, 80%, and 100%. For each ω_{ef} value we calculated the lengths of simulated movement paths for different phase angles between the moving spots. Fig. 8 shows the resulting path lengths as a function of phase angle for the different ω_{ef} values, and the perceived path according to our experimental findings. ω_{ef} value of 100% indicates that the motor signal balances the visual signal coming from the eyes, resulting in a nearly perfect compensation for the pursuit eye movements. The resulting path length in this case is nearly constant for all phase angles, as are the real movement paths of the non-pursued spot (circles of equal diameter; Fig. 6a). When the efferent signal was eliminated ($\omega_{ef} = 0$), MST units responded according to the retinal movement path, and the path length increased with phase angle according to the dependency of the retinal movement path on the phase angle (Fig. 6b). We see that 80% ω_{ef} yielded movement paths that are in

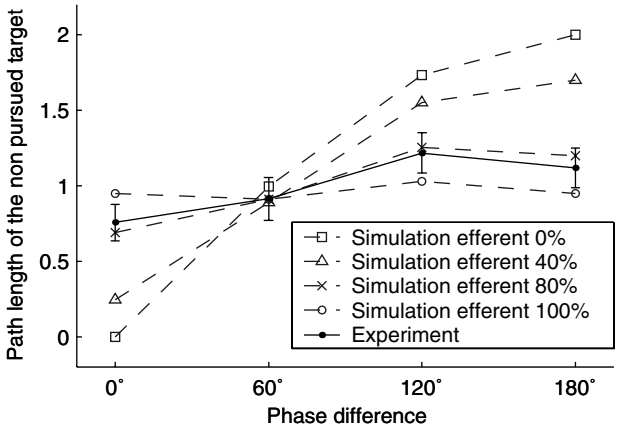

Fig. 8. Movement path length of the non-pursued target as a function of phase difference for two circularly spots moving in the same direction (Fig. 6). The graph shows simulated values for different ratios (0%, 40%, 80%, and 100%) between the efferent and afferent signal, and the experimental results. Path lengths are normalized to the perimeter of movement path of the targets during fixation.

good agreement with experimental findings. Simulation with other ω_{ef} values gave ratios between path length and phase which are not consistent with psychophysical findings.

4.3. Perceived path of a rotating target during circular pursuit in the opposite direction—simulation and psychophysical results

In the present section we deal with two light spots moving in the dark with the same angular velocity, along circles of the same diameter, but in opposite directions, while one of the targets (target A) is being pursued. Fig. 9a depicts the objective movement of the two targets. If pursuit is perfect, the retinal image of the non-pursued target (target B) moves sinusoidally along a straight line whose inclination depends on the phase difference between the two targets (Fig. 9b).

Again, due to the fact that tracking during pursuit is not perfect, the estimated retinal paths depicted in Fig. 9c differ slightly from the idealized retinal paths of Fig. 9b; the actual retinal paths are not straight lines, but highly eccentric ellipses, with inclinations close to those of Fig. 9b.

We simulated the network response, assuming perfect pursuit, for phase differences of 0°, 60°, 120°, and 180° with an 80% ω_{ef} strength. Fig. 10 shows, as an example, MST population response at six simulation time steps, for a 60° phase difference. MST population response was interpreted in terms of target B movement and the resulting movement paths are shown in Fig. 9d.

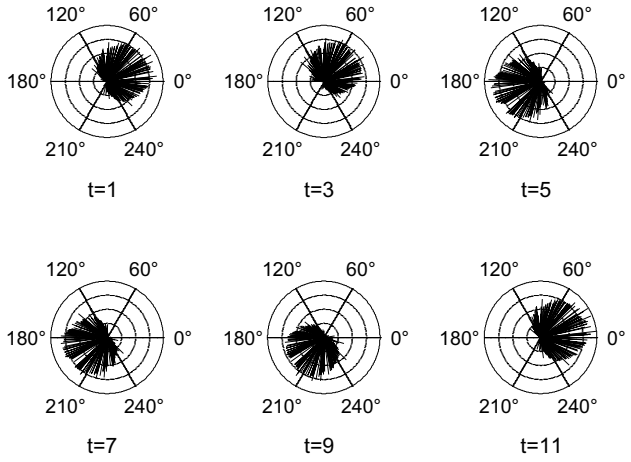

Fig. 10. Simulated MST population response of a circularly moving target, at six different time steps, during pursuit of a second target moving in the opposite direction at a 60° phase difference. Responses are normalized relative to the maximal response.

Fig. 9e shows the mean perceived movement paths obtained in our experiments. Subjects perceived target B as moving along an elongated ellipse with an inclination that increased with increase in phase difference. Simulation results (Fig. 9d) closely resembled the experimental findings (Fig. 9e) but differed dramatically from target B retinal path (Fig. 9b and c). The path

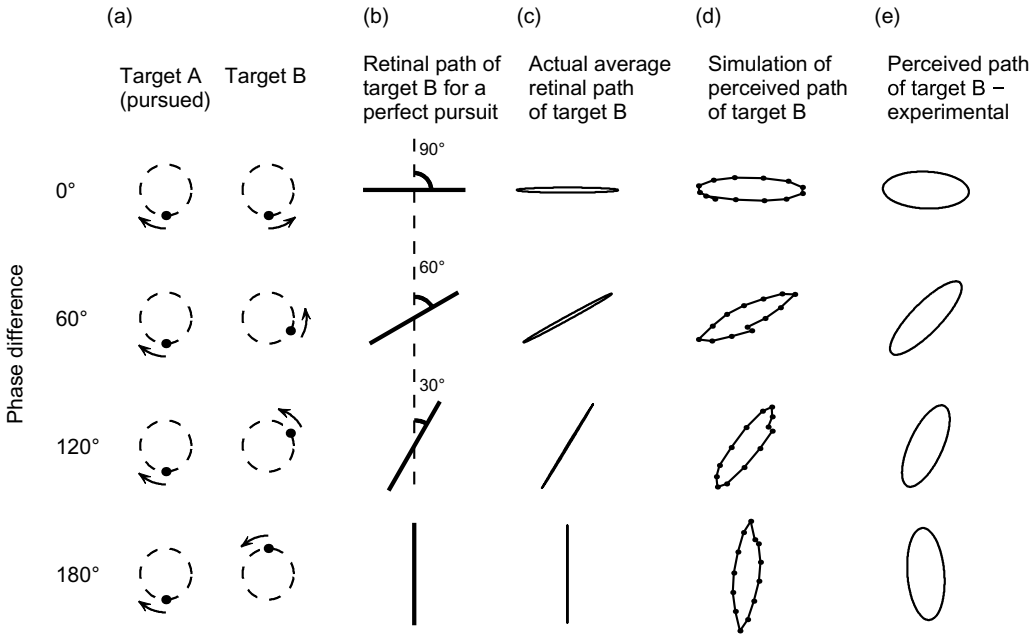

Fig. 9. Perceived movement path of a circularly moving spot during pursuit of a second spot moving in the opposite direction. (a) Objective movement of the two spots. Target A (pursued) moves clockwise along a circular path. Target B (non-pursued) moves counterclockwise, at different phases, along a circle of the same size. (b) Retinal image movement of target B for a perfect pursuit. (c) Estimated actual retinal image movement of target B, calculated according to average experimental pursuit gains. (d) Simulated movement path of target B represented by the MST population. (e) Experimental results of perceived movement of target B.

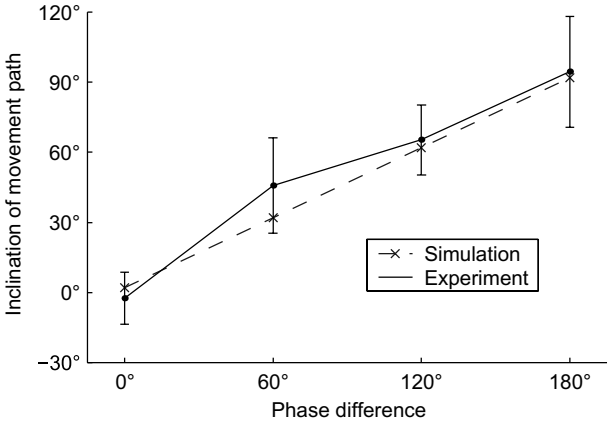

Fig. 11. Movement path inclination of the non-pursued target B as a function of phase difference between oppositely moving targets A (pursued) and B (Fig. 9). Dashed line: simulation results. Solid line: experimental results.

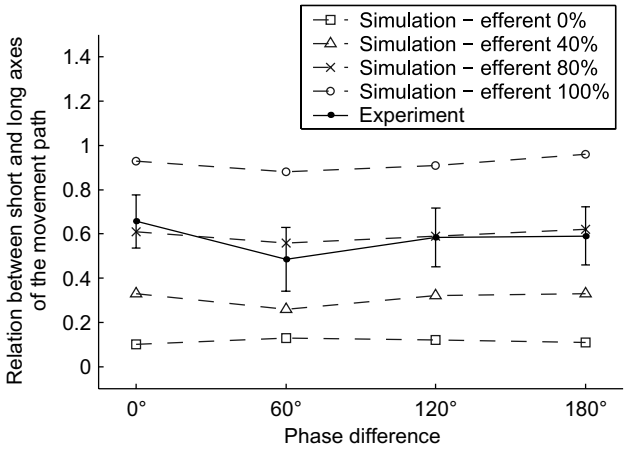

Fig. 12. Ratio between short and long axes of movement path of the non-pursued target as a function of the phase difference for two circularly spots moving in opposite directions (Fig. 9). Solid lines show simulated values for different efferent signal strengths: 0%, 40%, 80%, and 100%. The dashed line shows the experimental results.

inclinations, however, were similar for all conditions (Fig. 9b–e).

We compared how well did the ellipse inclination in our simulation fit experimental data; Fig. 11 shows the inclination of the ellipses as a function of phase difference for simulation (dashed line) and experimental results (solid line). As can be seen, the fit between the two conditions is quite good and both simulation and experimental results are very close to the retinal path inclinations (Fig. 9b and c).

In the simulations presented above we assumed that the efferent signal was 80% of the afferent one. To study the effect of the relative strength of the efferent signal, the previous simulations were repeated with four ω_{ef} values: 0%, 40%, 80%, and 100%. For each ω_{ef} value we calculated the lengths of simulated movement paths for different phase angles between the moving spots. Fig. 12 shows the relation between the short and long ellipse axes of the perceived movement path of target B as a function of the phase difference between the targets. Both simulation and experimental results for different ω_{ef} values are shown. For a 100% ω_{ef}, where there is nearly a perfect compensation for the pursuit eye movements, the resulting axes ratio is nearly 1 for all phase angles, in accordance with the real circular movement path of the non-pursued target. When the efferent signal was eliminated ($\omega_{ef} = 0$), MST units responded according to the retinal movement along a straight lines, resulting in nearly a 0 ratio between the short and long axes. As can be seen, an 80% ω_{ef} value yielded axes ratios in agreement with experimental findings. Simulation with other ω_{ef} values gave results inconsistent with psychophysical findings.

We note that the experimental findings shown in Fig. 12 do not indicate a monotonically decreasing relation between the axes ratio and the phase difference. That is, we did not find that the perceived ellipse became narrower as the phase difference increased, as reported by Kano and Hayashi (1981).

4.4. Perceived movement path during pursuit—analysis of underlying physiological mechanisms

When perception of a simple stimulus—a circularly moving object during fixation—was simulated, the resultant path, which coincided with the perceived one, is readily explained. The model V1 units represented local retinal movements, MT units represented patterns of retinal movements, and MST units responses could be interpreted in terms of perceived movement paths.

In the case of two moving spots, the non-veridical percept of the non-tracked spot was nicely predicted by the model and it is possible to relate this perception to the underlying physiological mechanisms by analyzing the model behavior. In the following discussion, we assume, as we did in the simulations, a perfect tracking of the pursued target.

In the case where the two targets moved in the same direction (Fig. 6) we take, for example, the condition of 180° phase difference, when pursued target A is at the bottom of its movement path, moving to the left (180° direction) at a v_0 velocity, and target B is at the top of its path moving to the right (0°) at v_0. Due to pursuit eye movements, target B retinal image moves to the right (0°) at $2v_0$ (see Fig. 13a) and excites V1 and MT units selective to movement directions about 0° and velocities about $2v_0$. MT units activate in turn MST units selective to directions about 0°, while MST units with ~180° preferred directions receive inhibitory input from MT. Unlike MT units, MST units also receive an input representing eye movements; at the same time step, eye-movement units responding to directions about

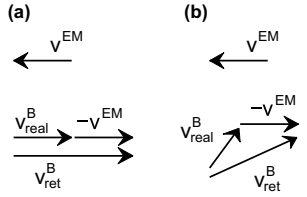

Fig. 13. Schematic diagram of momentary eye-movement vector and non-pursued target movement vector at two stimulus conditions. (a) Two targets moving in the same direction with a 180° phase difference, when pursued target A is at the bottom of its movement path (see Fig. 7a). (b) Two targets moving in opposite directions with a 60° phase difference, when pursued target A is at the bottom of its movement path (Fig. 10a). $\mathbf{v}^{EM}$—eye movement; $\mathbf{v}^{B}_{real}$—actual movement of the non-pursued target B; $\mathbf{v}^{B}_{ret}$—target B retinal image movement.

180° and velocities v_0 are activated. These units provide an excitatory input to MST units preferring ~180° directions, and an inhibitory input to MST units preferring ~0° directions. Note that the two sources of input to MST are not equally effective. Input from either MT or eye-movement representation is linearly dependent on velocity which is $2v_0$ in the MT case and v_0 in the eye-movement case. Since the eye-movement input was assumed to be 80% of the visual one, the eye-movement input to MST is about 0.4 of the visual one. The resulting MST population response (Fig. 7, $t = 1$) represents movement at 0° at a velocity between v_0 and $2v_0$. The same principle holds for other time steps and the movement path constructed from MST population response (Fig. 6d, bottom) is therefore larger than the real movement path, corresponding to v_0, yet smaller than the retinal movement path, corresponding to $2v_0$.

A similar analysis can be applied to the case where the two targets moved in opposite directions (Fig. 9b). We take, for example, the condition of 60° phase difference, when pursued target A is at the bottom of its movement path, moving to the left (180° direction) at v_0 velocity, and target B is moving in a 60° direction at v_0. Target B retinal image moves in a 30° direction at $\sqrt{3}v_0$ velocity (Fig. 13b), and this movement excites V1 and MT units with similar preferred directions and velocities. MT units excite, in turn, MST units selective to directions of about 30°, and inhibit MST units with ~210° preferred directions. At the same time step, eye-movement units responding to directions around 180° and velocities around v_0 are activated. These units provide an excitatory input to MST units preferring ~180° directions, and an inhibitory input to MST units preferring ~0° directions. As in the previous case, the two sources of input to MST were not equally effective, since MT input is proportional to $\sqrt{3}v_0$ while the eye-movement units input is proportional to v_0, and the latter was assumed to be 80% of the visual one. Consequently, the eye-movement input to MST is about 0.46 of the visual one and the resulting MST population response (Fig. 10, $t = 1$) represents an approximately 35° movement. This movement direction is different from the retinal (30°) or the real one (60°). The same principle holds for other time steps and the movement path reconstructed from MST units population response (Fig. 9d, 60° phase) is elliptical.

5. Discussion

The interaction between retinal motion signals and eye-movement-related motor signals, is evident in a host of perceptual phenomena. In this paper we investigated a complex perceptual phenomenon where tracking one object causes a non-veridical perception of a second, untracked object. Our neural network model of motion processing enabled us to suggest an explanation for this phenomenon in terms of underlying physiological mechanisms and to estimate the contribution of the motor signal to motion perception.

5.1. Modeling perceived movement during pursuit

Early models of perception during smooth pursuit (Gregory, 1958; Von Helmholtz, 1909; Von Holst, 1954) could not rely on relevant physiological data, and were rather schematic, not going beyond suggesting a subtraction of motion signals from the retinal ones. More recently, a wealth of physiological evidence on possible roles of cells, at the various cortical areas, in motion perception has been gathered. Direction selective cells in V1 (Dow, 1974; Hubel & Wiesel, 1968; Snodderly & Gur, 1995) project to area MT which is specialized in processing visual motion (Albright, 1984; Movshon & Newsome, 1984). MT projects to area MST where cells sensitive to object motion during pursuit were found (e.g. Erickson & Thier, 1991; Ferrera & Lisberger, 1997; Kawano et al., 1994; Komatsu & Wurtz, 1988; Squatrito & Maioli, 1997). Some MST cells apparently receive extra retinal input related to pursuit eye movements, enabling them to respond to object motion regardless of the eyes being in motion or stationary (Newsome, Wurtz, & Komatsu, 1988). Two recent models of smooth pursuit incorporated physiological data in their description of MST functioning. Dicke and Thier (1999) modeled the role of MST in pursuit generation and maintenance. The model units responded to retinal image slip as well as to eye and head velocity with similar preferred directions and the authors suggested that such cells are able to reconstruct target motion in world-centered coordinates, and to account for salient properties of visually guided pursuit. Their work deals mainly with the execution of pursuit eye and head movements, so that the model does not go into details of motion representation in V1 and MT.

Pack et al. (2001) proposed a neural model dealing with pursuit related cells in the ventral and dorsal subdivisions of MST, hypothesized to process target velocity and background motion. Similar to early studies, the model assumes a subtraction of extraretinal information about the velocity of eye rotation from retinal information about target velocity. The model addresses a number of behavioral phenomena related to velocity of pursuit eye movements and perceptual estimation of target and image velocities. Their model assumes, for simplicity, that movements are uni dimensional (leftward and rightward) and focuses on velocity as the central parameter.

Integration of retinal and extraretinal signals becomes a more complex process when two-dimensional movements are considered. Analytically, vectorial subtraction of the two signals is plausible. However, when biological reality is considered, implementing such a subtraction is far from being simple, unless some major non-physiological simplifications such as cells with non-realistic direction tuning properties, no separation between excitatory/inhibitory synapses, and single velocity movements are assumed.

To bring modeling a step closer to biological reality we developed a model (Furman & Gur, 2003) that simulated physiological activity in three cortical areas, V1, MT and MST. The model includes a full representation of direction and velocity of motion in V1 and MT and connections to MST that were developed by unsupervised learning which is more in line with physiological reality (cf. Albright, 1984; Hubel & Wiesel, 1968; Komatsu & Wurtz, 1988; Newsome et al., 1988). MST also received input from units representing eye-movement signal. The model thus enables us to understand and predict, in physiological terms, the perceptual outcome of simple or complex pursuit. In the examples described in the Results, it was thus possible to see how the non-tracked object retinal motion stimulates V1 and MT cells having appropriate velocity and direction selectivities, and how MT cells' excitatory and inhibitory inputs interact to determine MST responses. Finally, it was possible to follow how MST cells combine MT inputs with eye-movement signals, leading to MST population responses that corresponded nicely to perceptual data.

5.2. Model assumptions

One fundamental assumption of our study is that shape-from-motion perception during pursuit is based on integration of velocity signals. Since the main physiological pathway selective for motion is the V1/MT/MST one, it is reasonable that judgments of motion-generated-shape are largely based on integration of velocity signals performed in this pathway. Our focus on the motion processing stream is consistent with the strong activation in the motion pathway seen during pursuit related tasks (e.g Tikhonov, Haarmeier, Thier, Braun, & Lutzenberger, 2004) and with Lee and Blake (1999) study showing that shape can be generated solely from temporal signals. Within the motion pathway, area MST has been shown to receive an effective extra-retinal signal encoding eye movements. We thus interpret MST population responses as coding for the perceived shape-from-motion during pursuit. Unlike shape-from-motion, common (static) shape perception is based on simultaneous activation of many visual field loci and is presumably processed through the ventral, ''what'', pathway. How much do such position signals contribute to shape-from-motion perception during pursuit is not known, and it would be of interest to study modulation by pursuit eye movements of position selective cells in the ventral stream. The possible contribution of position signals was not included in our model. Thus, our estimate of the amount of compensation for the eye movements of pursuit is correct to the degree that the above assumptions are correct.

Our model also does not incorporate the findings that MST units' activity is modulated by eye position (Bremmer, Ilg, Thiele, Distler, & Hoffmann, 1997; DeSouza, Dukelow, & Vilis, 2002; Ilg & Thier, 2003; Squatrito & Maioli, 1997). This was done because position sensitivity in MST is relatively low, and it is likely that these position signals are more relevant to large eye and image movements.

Another simplifying assumption in our model concerns speed representation in area MST. According to some studies (Kawano et al., 1994; Tanaka et al., 1993), most MST units show a graded response to velocity. As an approximation we assumed that MST units respond linearly to velocity. However, a variety of speed tuning curves is observed in MST and often, speed selectivity differs during pursuit and during fixations (Chukoskie & Movshon, 2001). Therefore, the relation between speed judgments and population response in MST is still unclear.

5.3. Participation of the efferent signal in the perceptual process

One of the basic questions related to pursuit is the degree of participation of the efferent (motor) signal in the perceptual process. The research dealing with this is more than a century old; Dodge (1904) concluded that the perceptual system had practically no information on smooth pursuit eye movements. Carr (1907) disagreed with Dodge and the controversy seems not to have been resolved (Carr, 1935; Dodge, 1910). The extent to which the visual system compensates for smooth pursuit was addressed again by Stoper (1973) who concluded that compensation for pursuit was markedly low. Other experimental studies indicate a significant participation of eye-movement signals in the perceptual pro-

cess. One of the classical pursuit-related phenomena is the Aubert–Fleischl phenomenon: a reduction of the perceived velocity of a pursued object moving in the fronto-parallel plane in relation to the perceived speed during fixation. Most studies of this phenomenon show a reduction of about 30% in perceived speed during pursuit, indicating about 70% compensation (Aubert, 1886; Dichgans, Wist, Diener, & Brandt, 1975; Fleischl, 1882; Gibson, Smit, Steinschneider, & Johnson, 1957). Mack and Herman (1972) reported only a 10% reduction in the perceived extent of motion of a pursued target, but this may be an overestimation due to inaccurate pursuit during the initial phase of target movement. Coren, Bradley, Hoenig, and Girgus (1975) estimated that there was a high degree of compensation for eye movements.

By simulating the psychophysical experiments for targets moving in the same and in opposite directions, with different values of ω_{ef}, it was possible to estimate the relative contribution of the efferent signal. For two targets moving in the same direction, the simulated movement path of the non-pursued target was always circular but the path diameter which varied with phase difference, strongly depended on ω_{ef}. For a ω_{ef} value of about 80%, the simulated path lengths were in accordance with psychophysical findings while other ω_{ef} values, representing a weaker efferent signal in relation to the afferent one, or balanced efferent and afferent signals, led to model predictions inconsistent with experimental data (Fig. 8). For two targets moving in opposite directions, the simulated perceived movement path of target B was an ellipse, whose inclination depended on the phase difference. While the inclinations were independent of ω_{ef}, the ellipse's shape clearly depended on ω_{ef}. Again, only ω_{ef} values about 80% yielded simulation results consisted with psychophysical findings (Fig. 12). The model thus supports the claim that the efferent signal participates in a significant way in the process, yet is smaller in magnitude than the afferent signal. It should be noted that in natural viewing, it is possible that the relation between afferent and efferent signals varies with the attributes of the visual stimuli (such as size or contrast; c.f. Crowell & Andersen, 2001).

Why is compensation incomplete, leading us to perceive non-veridical movements during pursuit? Post and Leibowitz (1985) suggested that underestimation of target velocity during pursuit results from activation of the smooth component of the reflexive eye-movement system, so that a weaker efferent signal is needed to maintain pursuit, resulting in a lower perceived velocity. It is also possible that during the evolvement of the pursuit system in foveated species there was an adaptive need for pursuit compensation. It is evident, however, that the visual system can function well with less than perfect compensation, so there was no adaptive pressure to improve compensation accuracy. Another possible explanation for the partial pursuit compensation may relate to the fact that unlike the present study, in natural viewing we often pursue objects moving in depth, surrounded by complex stimuli, during head and body movements. All these aspects of the visual scene interact during pursuit, and the complex non-linear integration process of the different signals may constrain the efferent signal to be lower relative to the visual one.

Acknowledgement

The authors would like to thank the two anonymous reviewers for valuable input.

References

Albright, T. D. (1984). Direction and orientation selectivity of neurons in visual area MT of the macaque. *Journal of Neurophysiology, 52*, 1106–1130.

Aubert, H. (1886). Die bewegungsempfindungen. *Pflügers Archiv, 39*, 347–370.

Bremmer, F., Ilg, U. J., Thiele, A., Distler, C., & Hoffmann, K. P. (1997). Eye position effects in monkey cortex. I. Visual and pursuit-related activity in extrastriate areas MT and MST. *Journal of Neurophysiology, 77*, 944–961.

Carr, H. A. (1907). The pendular whiplash illusion of motion. *Psychological Review, 14*, 169–180.

Carr, H. A. (1935). *An introduction to space perception*. New York: Green and Co.

Chukoskie, L., & Movshon, J. A. (2001). Neural representations of speed during smooth pursuit eye movements. *Journal of Vision, 1*, 403 (Abstract).

Coren, S., Bradley, D. R., Hoenig, P., & Girgus, J. S. (1975). The effect of smooth tracking and saccadic eye movements on the perception of size: The shrinking circle illusion. *Vision Research, 15*, 49–55.

Crowell, J. A., & Andersen, R. A. (2001). Pursuit compensation during self-motion. *Perception, 30*, 1465–1488.

DeSouza, J. F. X., Dukelow, S. P., & Vilis, T. (2002). Eye position signals modulate early dorsal and ventral visual areas. *Cerebral Cortex, 12*, 991–997.

Dichgans, J., Wist, E., Diener, H. C., & Brandt, T. (1975). The aubert fleischl phenomenon: A temporal frequency effect on perceived velocity in afferent motion percetion. *Experimental Brain Research, 23*, 529–533.

Dicke, P. W., & Thier, P. (1999). The role of cortical area MST in a model of combined smooth eye-head pursuit. *Biological Cybernetics, 80*, 71–84.

Dodge, R. (1904). The participation of eye movements in the visual perception of motion. *Psychological Review, 11*, 1–14.

Dodge, R. (1910). The pendular whiplash illusion. *Psychological Bulletin, 7*, 390–394.

Dow, B. M. (1974). Functional classes of cells and their laminar distribution in monkey visual cortex. *Journal of Neurophysiology, 37*, 927–946.

Erickson, R. G., & Thier, P. (1991). A neuronal correlate of spatial stability during periods of self-induced visual motion. *Experimental Brain Research, 86*, 608–616.

Ferrera, V. P., & Lisberger, S. G. (1997). Neuronal responses in visual areas MT and MST during smooth pursuit target selection. *Journal of Neurophysiology, 78*, 1433–1436.

Festinger, L., Sedgwick, H. A., & Holtzman, J. D. (1976). Visual perception during smooth pursuit eye movements. *Vision Research, 16*, 1377–1386.

Filehne, W. (1922). Über das optische wahrnehmen von bewegungen. *Zeitschrift für Sinnesphysiologie, 53*, 134–144.

Fleischl, E. V. (1882). Physiologisch optische notizen. *Sitzungsaberichte der Kais. Akademie der Wissenschaften in Wien, 3*, 7–25.

Furman, M., & Gur, M. (2003). Self-organizing neural network model for motion processing in the visual cortex during smooth pursuit. *Vision Research, 43*, 2155–2171.

Gibson, J. J., Smit, O. W., Steinschneider, A., & Johnson, C. W. (1957). The relative accuracy of visual perception of motion during fixation and pursuit. *American Journal of Psychology, 70*, 64–68.

Gregory, R. L. (1958). Eye movements and the stability of the visual world. *Nature, 182*, 1214–1216.

Hebb, D. O. (1949). *The organization of behavior*. New York: Wiley.

Hubel, D. H., & Wiesel, T. N. (1968). Receptive fields and functional architecture of monkey striate cortex. *Journal of Physiology (London), 195*, 215–243.

Ilg, U. J., & Thier, P. (2003). Visual tracking neurons in primate area MST are activated by smooth-pursuit eye movements of an "imaginary" target. *Journal of Neurophysiology, 90*, 1489–1502.

Kano, C., & Hayashi, K. (1981). The apparent path of a stationary and circularly moving spot during the smooth pursuit of another circularly moving spot. *Acta Psychologica, 48*, 151–160.

Kawano, K., Shidara, M., Watanabe, Y., & Yamane, S. (1994). Neural activity in cortical area MST of alert monkey during ocular following responses. *Journal of Neurophysiology, 71*, 2305–2324.

Komatsu, H., & Wurtz, R. H. (1988). Relation of cortical areas MT and MST to pursuit eye movements. I. Localization and visual properties of neurons. *Journal of Neurophysiology, 60*, 580–603.

Lee, S., & Blake, R. (1999). Visual form created solely from temporal structure. *Science, 284*, 1165–1168.

Mack, A., & Herman, E. (1972). A new illusion: The underestimation of distance during pursuit eye movement. *Perception and Psychophysics, 12*, 471–473.

Movshon, J. A., & Newsome, W. T. (1984). Functional characteristics of striate cortical neurons projecting to MT in the macaque. *Society for Neuroscience Abstract, 10*, 993.

Newsome, W. T., Wurtz, R. H., & Komatsu, H. (1988). Relation of cortical areas MT and MST to pursuit eye movements. II. Differentiation of retinal from extraretinal inputs. *Journal of Neurophysiology, 60*, 604–620.

Oja, E. (1982). A simplified neuron model as a principal component analyzer. *Journal of Mathematical Biology, 15*, 267–273.

Pack, C., Grossberg, S., & Mingolla, E. (2001). A neural model of smooth pursuit control and motion perception by cortical area MST. *Journal of Cognitive Neuroscience, 13*, 102–120.

Post, R. B., & Leibowitz, H. W. (1985). A revised analysis of the role of efference in motion perception. *Perception, 14*, 631–643.

Rottach, K. G., Zivotofsky, A. Z., Das, V. E., Averbuch-Heller, L., Discenna, A. O., Poonyathalang, A., & Leigh, R. J. (1996). Comparison of horizontal, vertical and diagonal smooth pursuit eye movements in normal human subjects. *Vision Research, 36*, 2189–2195.

Snodderly, D. M., & Gur, M. (1995). Organization of striate cortex of alert, trained monkeys (macaca fascicularis) ongoing activity, stimulus activity, and widths of receptive field activating regions. *Journal of Neurophysiology, 74*, 2100–2125.

Squatrito, S., & Maioli, M. G. (1997). Encoding of smooth pursuit direction and eye position by neurons of area MSTd of macaque monkey. *Journal of Neuroscience, 17*, 3847–3860.

Stoper, A. E. (1973). Apparent motion of stimuli presented stroboscopically during pursuit movement of the eye. *Perception and Psychophysics, 13*, 201–211.

Tanaka, K., Sugita, Y., Moriya, M., & Saito, H. A. (1993). Analysis of object motion in the ventral part of the medial superior temporal area of the macaque visual cortex. *Journal of Neurophysiology, 69*, 128–142.

Tikhonov, A., Haarmeier, T., Thier, P., Braun, C., & Lutzenberger, W. (2004). Neuromagnetic activity in medial parietooccipital cortex reflects the perception of visual motion during eye movements. *Neuroimage, 21*, 593–600.

Von Helmholtz, H. (1909). *Handbuch der physiologischen Optik*. Hamburg: Voss.

Von Holst, E. (1954). Relations between the central nervous system and the peripheral organs. *British Journal of Animal Behaviour, 2*, 89–94.